Environment International 122 (2019) 357–362

Contents lists available at ScienceDirect

Environment International

journal homepage: www.elsevier.com/locate/envint

Synthesis of MgO-coated corncob biochar and its application in lead stabilization in a soil washing residue

Zhengtao Shen[a,b,c,1], Jingzhuo Zhang[a,b,1], Deyi Hou[a,b,*], Daniel C.W. Tsang[d], Yong Sik Ok[e], Daniel S. Alessi[c]

[a] School of Environment, Tsinghua University, Beijing 100084, China
[b] National Engineering Laboratory for Site Remediation Technologies, Beijing 100015, China
[c] Department of Earth and Atmospheric Sciences, University of Alberta, Edmonton T6G 2E3, Canada
[d] Department of Civil and Environmental Engineering, Hong Kong Polytechnic University, Hung Hom, Kowloon, Hong Kong, China
[e] Korea Biochar Research Center, O-Jeong Eco-Resilience Institute (OJERI), Division of Environmental Science and Ecological Engineering, Korea University, Seoul 02841, Republic of Korea

ARTICLE INFO

Keywords:
Engineered biochar
Magnesium oxide (MgO)
Biochar-mineral composite
Lead immobilization
In situ stabilization
Soil remediation

ABSTRACT

In this study, a magnesium oxide (MgO) coated corncob biochar (MCB) was synthesized by pyrolyzing $MgCl_2$ pretreated corncob, for a better performance in lead immobilization in a contaminated soil compared with corncob biochar (CB). The properties and microstructures of CB and MCB were investigated. It was observed that MgO particles ranging from 1 to 2 μm were well coated on MCB, and the MgO content in MCB was calculated at 29.90% in w/w. The surface area of the biochar was significantly enhanced from 0.07 to 26.56 m^2/g after the MgO coating. The MgO coating also significantly facilitated the lead removal percentage from 23% to 74% in aqueous solution by biochar. CB failed to immobilize lead in a soil washing residue and could not reduce its environmental risks in a laboratory incubation study. In contrast, MCB was applied to the soil and resulted in a significant reduction in TCLP leached lead from 10.63 to 5.24 mg/L (reduced by 50.71%). The comparison between MCB and other amendments suggests that the biochar component of MCB adsorbed lead onto its surface through cation-π interaction and increased surface adsorption due to higher surface area, and then the MgO coated on MCB's surface further enhanced the adsorption through precipitation. The synergistic roles of biochar-mineral composites make them a promising candidate for soil remediation.

1. Introduction

Soil contamination is becoming a severe problem in developing countries (e.g., China and India), which affects human health, economic growth and social development (Zhao et al., 2015; Shen et al., 2018a, 2018b, 2018c; Hou and Li, 2017). China released the "Action plan on prevention and control of soil pollution" recently and showed a huge ambition to deal with the problem of soil contamination (Zhang and Li, 2016). Stabilization is regarded as one of the most effective technologies to remediate heavy metal contaminated soil. In comparison with other traditional physical and chemical treatment technologies, soil stabilization tend to be cost-effective, versatile, and fast in implementation (Al-Tabbaa et al., 2012; Shen et al., 2018a, 2018b, 2018c; Wang et al., 2016). Moreover, soil stabilization renders smaller life cycle environmental footprint, and it can be considered a sustainable remediation approach (Hou et al., 2017a; O'Connor et al., 2018). Therefore, stabilization technology has a huge potential to be applied in soil remediation of heavy metals, the most widely distributed soil contaminants in China (Qu et al., 2016; Hou et al., 2017b).

One of the most important aspects for soil stabilization is to find effective and sustainable adsorptive/binding materials. Biochar has been widely regarded as a promising material for soil stabilization, due to its multiple benefits including metal immobilization, low-cost, reuse of waste materials with high availability, carbon storage and greening effect (Lehmann, 2007; Lehmann et al., 2008; Sohi, 2012; Shen et al., 2016b). Although biochar generally shows effective immobilization of heavy metals in soil (O'Connor et al., 2018), it has been observed that single biochar amendment may not necessarily reduce heavy metal mobility or bioavailability depending on soil texture and contamination conditions due to the limitation of its adsorption mechanisms (e.g.,

* Corresponding author at: School of Environment, Tsinghua University, Beijing 100084, China.
E-mail address: houdeyi@tsinghua.edu.cn (D. Hou).
[1] These authors contributed equally to this work.

https://doi.org/10.1016/j.envint.2018.11.045
Received 11 September 2018; Received in revised form 13 November 2018; Accepted 19 November 2018
Available online 28 November 2018

cation exchange) (Shen et al., 2016a, 2016b; Shen et al., 2018a).

Modification has been used to enhance the adsorption capacity of biochar for heavy metals, including chemical modifications, physical modifications, impregnation with mineral sorbents and magnetic modifications (Upamali et al., 2016). The modification of biochar has been extensively investigated to enhance its performance in water treatment (Mosa et al., 2016; Sizmur et al., 2017; Yang and Jiang, 2014). Few studies have has been carried out with a purpose of soil remediation. Therefore, it is important to find an effective modification for biochar to enhance its performance in heavy metal immobilization in soil.

In view of these considerations, an MgO-coated corncob biochar was synthesized and applied to a lead contaminated soil. The use of corncob to produce biochar was due to its high availability: corn (annual production of 2.06×10^8 t) is one the most abundant crops in China and approximately 3.7×10^7 t of corncob is generated annually (Liu et al., 2014; Vu et al., 2017). Magnesium oxide (MgO), a promising material with a huge potential and excellent performance in soil stabilization (Sanderson et al., 2015; Wang et al., 2016), was expected to significantly enhance the immobilization of heavy metals by corncob biochar. Therefore, the MgO-coated corncob biochar was synthesized and characterized, and its performance in lead immobilization in soil was investigated.

2. Materials and methods

2.1. Production and synthesis of biochar

The corncob was obtained from Biyang, Zhumadian, Henan province, China. Upon receipt, the corncob was oven dried at 60 °C to reach constant weight. The corncob was then smashed, ground and sieved through #20 (< 0.85 mm) mesh. Corncob biochar (CB) was produced in a furnace with limited air. The sieved corncob was heated at a heating rate of 10 °C/min to reach 600 °C (Zhang et al., 2012). The highest temperature (600 °C) was maintained for 1 h. The synthesis of MgO-coated corncob biochar (MCB) was based on Li et al. (2016) and Zhang et al. (2012). Briefly, the sieved corncob was mixed with 0.5 M magnesium chloride hexahydrate ($MgCl_2{\cdot}6H_2O$) at solid to liquid ratio of 1:20 g/mL and stirred intensely for 1 h. The mixture was then oven dried at 60 °C without filtration to reach a constant weight before the same biochar production process as CB. After production, the CB and MCB were sieved through #40 (< 0.425 mm) mesh and stored in sealed sample bags.

2.2. Biochar characterization

The pH of the biochars was determined using methods described in previous studies (Alam et al., 2018a, 2018b; Von Gunten et al., 2017). Briefly, a certain amount (0.1 g) of biochar was added to 10 mL of deionized water and shaken at 250 rpm for 24 h. After centrifugation, the pH of the supernatant was test by a pH meter. The Brunauer–-Emmett–Teller (BET) surface area of the biochars was determined by a Tristar II 3020 (Micromeritics). The C, H and N contents of biochar were tested by a CE-440 Elemental Analyzer (PERKIN ELMER). Other elements (e.g., Mg and Cl) were determined by a XRF-1800 (SHIMADZU).

The molecular structure of the biochars was examined by a VERTEX 70v Fourier transform infrared spectroscopy (FT-IR) spectrometer (BRUKER), and the wavenumber was from 4000 to 600 cm^{-1}. The crystalline phases of the biochar were identified by a D8 ADVANCE X-ray diffractometer (XRD) (Bruker). The dry samples were mounted on a flat holder and examined with a CuKα source operating at 40 kV and 40 mA, emitting radiation at a wavelength of 1.5406 Angstroms. The scanning regions were between 10 and 60° of 2θ values at a rate of 0.1 s/step and a resolution of 0.01°/step. The surface morphology of the biochars (coated with Pt) was tested by a SU8010 Ultra-High Resolution (1.0 nm) Scanning Electron Microscope (SEM) (Hitachi, Japan).

Table 1
Details of the amendments (MCB - MgO-coated corncob biochar, CB – corncob biochar).

No.	Amendment	Dosage (w/w)	Note
T1	Without amendment	0%	Control
T2	MCB	5%	
T3	MgO + $MgCl_2$ (MM)	2.7%	Equivalent to Mg contents in T2
T4	CB	2.3%	Equivalent to CB dosage in T2
T5	CB	5%	
T6	MM + CB	2.7% + 2.3%	Simple mix of MM and CB

(Note: the MM in T3 and T6 was produced through the same procedure as MCB but with the exclusion of corncob, and it is a mixture of MgO and $MgCl_2$; the elemental composition of MM is shown in Table S1)

2.3. Amendment and chemical analysis

The lead removal capacity of CB and MCB was investigated and compared. Briefly, 1 g of biochar was added to 20 mL solution of 5 mM $Pb(NO_3)_2$. The mixture was shaken at 250 rpm and centrifuged and filtered through a 0.45 μm filter. The concentrations of lead in the filtrate were measured by inductively coupled plasma/optical emission spectrometry (ICP-OES) (Perkin-Elmer, Optima 8300) after dilution (if necessary).

The performance of MCB in lead immobilization in soil was investigated and compared with other amendments (Table 1). The soil (Table 2) was a soil washing residue and its primary contaminant is lead (3410 mg/kg) (Shen et al., 2018a; Shen et al., 2018b). The details of the soil washing process can be found in our previous studies (Shen et al., 2018a; Shen et al., 2018b). The soil is alkaline with a pH of 9.14 and contains high clay content (89.68%). The lead in the soil exceeds the Toxicity Characteristic Leaching Procedure (TCLP) regulatory level, and single biochar amendment failed to significantly reduce its risks (Shen et al., 2018a). Therefore, MCB was applied to the soil to investigate whether the modification successfully improved the performance of CB in lead immobilization in the soil in comparison with other amendments. The dosage of the amendments was 5% in w/w and the water content was 40% by soil dry weight, based on the previous research (Shen et al., 2018a; Shen et al., 2018b). After the amendment, the soils were incubated under room temperature and ~100% relative humidity in a moisture chamber for 28 days.

After incubation, the soils were oven dried at 60 °C to reach constant weight. TCLP was performed to assess the mobility and environmental risks of lead in the soils based on USEPA 1311. Briefly, the soil and buffer solution (HOAc/NaOAc, pH 2.88) were mixed at a solid/liquid ratio of 1:20 in a 50-mL polyethylene tube. The extraction of pH 2.88 was selected based on the TCLP protocol “determination of appropriate extraction fluid”. The mixture was shaken at 250 rpm for 18 h before filtration. Lead concentrations in the filtrate were measured by ICP-OES

Table 2
Properties of soil washing residue (Shen et al., 2018a; Shen et al., 2018b).

Property	Value
pH	9.14
Total organic matter content (%)	3.46
Clay (0–002 mm) (%)	89.68
Silt (0.002–0.05 mm) (%)	10.21
Sand (0.05–2 mm) (%)	0
Pb (mg/kg)	3410
Al_2O_3 (%)	12.51
MnO (%)	3.36
S (%)	3.31
CaO (%)	1.44

Table 3
properties of corncob biochar (CB) and MgO-coated corncob biochar (MCB).

	CB	MCB
pH	7.17 ± 0.03	10.45 ± 0.01
BET surface area (m^2/g)	0.07	26.56
C (%)	82.95 ± 0.17	53.51 ± 0.25
H (%)	2.42 ± 0.16	4.187 ± 0.03
N (%)	0.56 ± 0.03	0.14 ± 0.01
Mg (%)	N.A.	21.74
Cl (%)	N.A.	11.25

(N.A.-not available)

after dilution (if necessary) and acidification.

2.4. Statistical analysis

The pH, elemental analyses and TCLP extraction were conducted in triplicates. Mean and standard deviations were reported for each experiment. The microstructural analyses were conducted once. The difference between two data groups was evaluated by two-tailed *t*-test at a significance level of 0.05. Different lower-case letters were used to indicate significant differences between two data groups in the figures. If the lower-case letters of two groups contain no same letters, it means the two groups are significantly different ($P < 0.05$). If they contain any same letter, it means they are not significantly different ($P \geq 0.05$). The statistical analysis was conducted using Microsoft Excel 2016.

3. Results and discussion

3.1. Biochar properties

The properties of the biochars are shown in Table 3. The pH of CB was 7.17, which is close to neutral. MgO coating significantly enhanced biochar pH to 10.45. The BET surface area of CB was very low (0.07 m^2/g), which was in line with previous findings on corncob biochars (Hao et al., 2013). Higher production temperatures could result in CB with higher surface areas (Hao et al., 2013), however pyrolysis at higher temperature would also render less functional groups on biochar and cause higher energy consumption and cost (Zhao et al., 2017a, 2017b). After MgO coating, the surface area of the biochar significantly increased to 26.56 m^2/g. A range of mechanisms can contribute to the increased surface area. The $MgCl_2$ has a strong dehydration ability towards the carbohydrate polymers in corncob which can enhance the release of volatile matter and aid the formation of open pores during pyrolysis at high temperatures (Liu et al., 2013). The formed MgO itself has a relatively high surface area (Jin and Al-Tabbaa, 2014). Therefore, the surface area of MCB was significantly enhanced compared with CB. This suggests that the MCB may have higher adsorption capacities for heavy metals than CB. The C content of CB was relatively high 82.95% while its H content was low (2.42%), suggesting a well developed aromatic structure for CB (Zhao et al., 2017a, 2017b). After MgO coating, the C content significantly decreased due to the dilution effect by the added amount of Mg and Cl on the biochar. The H content of MCB increased, which was likely due to the coated bischofite ($MgCl_2 \cdot H_2O$) on MCB, which will be illustrated in Section 3.2.

Approximately 21.74% (w/w) of Mg was observed in MCB, these Mg may be attributed to the MgO coated on MCB surface, however, this needs to be further verified by micro-structural analysis. It is of note that Cl (11.25%) was also observed in MCB, which was the residual $MgCl_2$ from the synthesis process. Similarly, the MgO + $MgCl_2$ (MM) in T3 and T6 contains 40.32% Mg and 37.05% Cl (Table S1). If attributing the presence of Cl to the formation of $MgCl_2$, then 12.52% Mg in the MM was associated with Cl based on stoichiometric calculation. If the remaining Mg (27.80%) was all in the form of MgO, the MgO purity in the MM can be calculated as 46.33%, while 49.57% was $MgCl_2$.

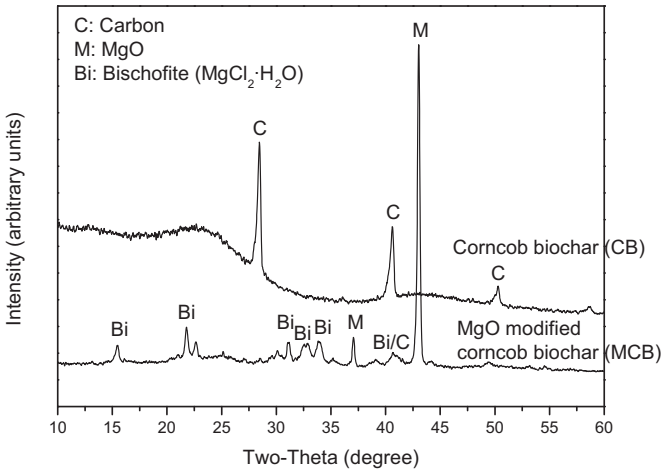

Fig. 1. XRD patterns of the corncob biochar and MgO-coated corncob biochar.

Similarly, the estimated MgO content of MCB can be calculated as 29.90%, and the $MgCl_2$ content of MCB can be calculated as 15.05%. Therefore, the coated MgO on MCB was actually mixed with $MgCl_2$, and the MM in T3 and T6 was also a mixture of MgO and $MgCl_2$. Previous research using $MgCl_2$ pretreated biomass to produce MgO-coated biochar did not report the $MgCl_2$ concentration in their produced MgO or MgO-coated biochars (Li et al., 2017; Liu et al., 2013; Zhang et al., 2012), therefore, the purity of produced MgO should be measured and taken into consideration in future studies.

3.2. Biochars microstructures

The XRD patterns of CB and MCB are shown in Fig. 1. The peaks at 28°, 41° and 50° from CB were typically observed from biochar and carbon-based materials (Hao et al., 2013; Keiluweit et al., 2010). After MgO coating, significant peaks of MgO (at 37° and 43°) were observed from MCB, suggesting that MgO was successfully coated on biochar surface. A range of peaks corresponding to bischofite ($MgCl_2 \cdot H_2O$) were also observed from MBC. This suggests that a certain amount of $MgCl_2$ remained on CB during synthesis, which is in line with the elemental analysis.

The FT-IR spectra of CB and MCB are shown in Fig. 2. For CB, the peak at 3034 cm^{-1} is assigned to aromatic C—H (Budai et al., 2017). The peak at 1575 cm^{-1} is ascribed to aromatic C=C (Budai et al., 2017; Keiluweit et al., 2010). The peak at 1111 cm^{-1} corresponds to C—O—C

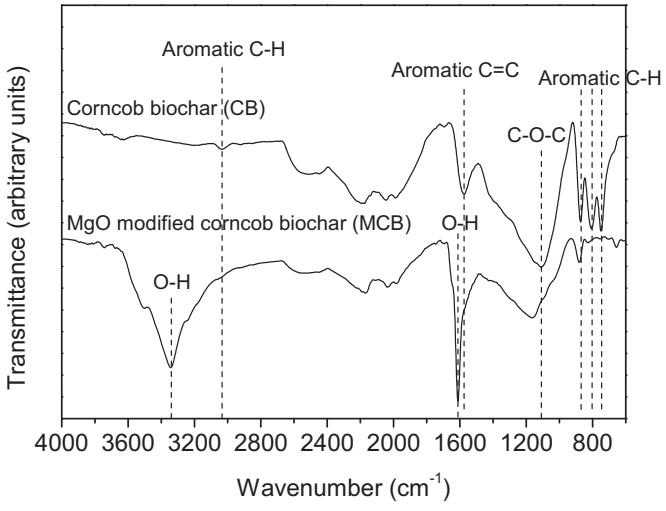

Fig. 2. FT-IR spectra of the corncob biochar and MgO-coated corncob biochar.

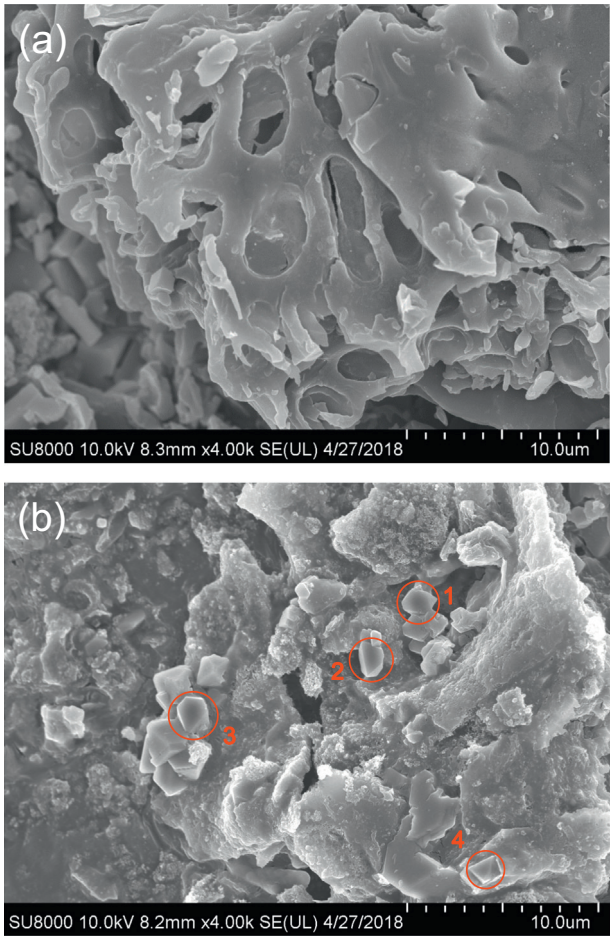

Fig. 3. SEM image of corncob (a) and MgO-coated corncob biochar (b), the EDX plots are shown in Fig. S1, S2, S3 and S4.

stretching vibrations in cellulose and hemicellulose, which was typically observed for corncob and other biochars (Budai et al., 2017; Keiluweit et al., 2010; Vu et al., 2017; Xin et al., 2017). Likewise, the peaks at 872, 806 and 748 cm^{-1} were frequently observed from corncob and other biochars representing aromatic C—H out-of-plane deformation. The FT-IR results generally show an active aromatic structure for CB. After MgO coating on MCB, the strong peaks at 3339 and 1612 cm^{-1} are attributed to O—H stretching vibration of hydrogen-bonded groups (Jung et al., 2015), which originated from the bischofite as shown in Fig. 1 and covered the original aromatic-associated peaks of CB at 3034 and 1575 cm^{-1}. The intensity of the peaks representing aromatic C—H at 872, 806 and 748 cm^{-1} was significantly reduced after MgO coating, suggesting that the MgO and bischofite had been coated on the aromatic structure.

The surface morphology of the biochars is shown in Fig. 3. Layered homogeneous sheets were observed on biochar surface (Fig. 3a), which was typical surface morphology for corncob derived biochars at relative high temperatures (Hao et al., 2013; Vu et al., 2017). Macro-pores are distributed on the sheets with diameters ranging from 1 to 6 μm, which is similar to the observation on corncob biochars produced at 550 °C (Hao et al., 2013). After MgO coating (Fig. 3b), it can be observed that hexagonal and cubic MgO particles with a size of 1–2 μm were well coated on the biochar surface (Bdewi et al., 2015), suggesting that a successful modification was achieved. Previous study, using a similar synthesis method for $MgCl_2$ pretreated biomass (sugar beet tailings, sugarcane bagasse, cottonwoods, pine woods or peanut shells), observed nanoscale MgO particles (19.6–66.9 nm) coated on biochar's surface. This suggests that the particle size of coated MgO on biochar

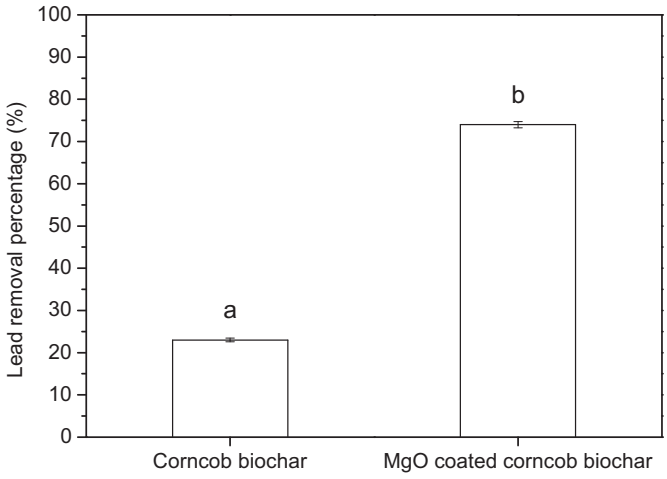

Fig. 4. Lead removal in aqueous solution by corncob biochar and MgO-coated corncob biochar (0.1 g biochar in 20 mL of 5 M lead solution; different lower-case letters indicate significant differences between two data groups).

may vary depending on influencing factors such as $MgCl_2$ concentration, feedstock type and laboratory conditions.

3.3. Performance of the biochars in soil amendment

Before application to the soil washing residue, the performance of lead removal in aqueous solutions for the biochars was investigated. It can be observed from Fig. 4 that the MgO coating significantly increased the adsorption capacity of the biochar. The lead removal percentage increased from 23% to 74% after MgO coating.

The MCB was then applied in a lead contaminated soil and compared with other amendments. It can be observed (Fig. 5) that the original soil (T1) exceeded the TCLP regulatory limit and poses great environmental risks. Single CB treatments (T4 and T5) had insignificant influence on heavy metal immobilization, whereas MCB amendment (T2) significantly reduced the TCLP leached lead to approximate the regulatory level: from 10.63 to 5.24 mg/L (reduced by 50.71%).

The performance of MCB was compared with MM (equivalent to the Mg content in MCB). It can be found that MCB was much more effective than MM amendment (T3) in reducing lead leachability in the soil. The performance of MCB was also compared with simple mix of CB and MM (equivalent to the CB and Mg contents in MCB, respectively). It is

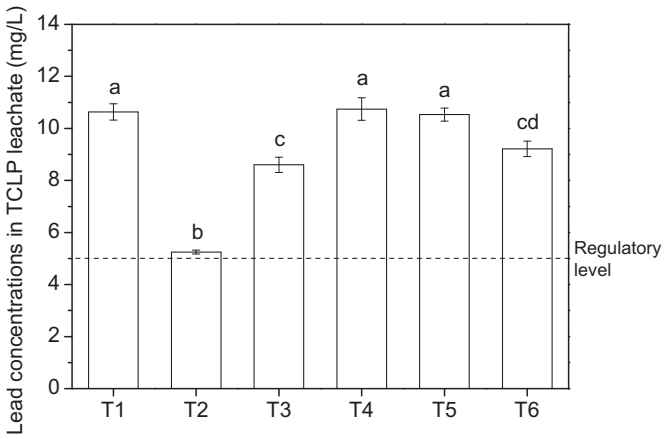

Fig. 5. Lead concentrations in TCLP leachate among different amendments (T1-control, T2-MgO-coated corncob biochar (5%), T3-Produced MgO (2.7%), T4-biochar (2.3%), T5-biochar (5%), T6-Produced MgO (2.7%) + biochar (2.3%); different lower-case letters indicate significant differences between two data groups).

noteworthy that MCB also performed much better in lead immobilization in the soil than simple mix of CB and MM (T6). Therefore, it can be concluded that the MgO coating has enhanced the performance of both CB and MgO in lead immobilization in the soil.

3.4. Discussion and limitation

There may be two reasons why single CB amendment failed to significantly reduce the TCLP leached lead in the soil. One is that CB failed to competitively adsorb the lead when compared to the clay particles in the soil washing residue, and therefore actually has little effect on the lead mobility in the soil. Another is that biochar adsorbed a certain amount of lead to its surface, however the adsorbed lead was leached out under TCLP condition. The CB has active aromatic structure which can adsorb lead through cation-π interaction (Shen et al., 2017), however the adsorbed lead may be leached out under low pH conditions (e.g., TCLP leachate).

Single MM amendment slightly reduced the TCLP leached lead (from 10.63 to 9.22 mg/L, a reduction of 13.26%), which was much less significant than that of MCB (a reduction of 50.71%). This suggests that, although CB alone failed to significantly reduce the TCLP leached lead, after MgO coating, the biochar component plays an important role in aiding MgO's immobilization of lead in the soil. The potential mechanisms may be that the biochar component in MCB adsorbed lead onto its surface through cation-π interaction. Then the MgO coating on the biochar surface further enhanced the adsorption through precipitation (e.g., $Pb(OH)_2$ and $Pb_3(CO_3)_2(OH)_2$), which is the main mechanism for MgO to immobilize metals (Suzuki et al., 2013).

Single MM amendment may result in the aggregation of MgO particles, which reduces their effective contact with lead. Therefore, their immobilization efficiency was reduced. After coating on biochar, MgO particles were evenly distributed on biochar surface (Fig. 3), and therefore effectively contact with lead cations in soil and immobilize them through precipitation. In addition, the MgO coating process significantly increased the surface area of biochar, which enhanced MCB's adsorption of lead by creating more binding sites.

It is of note that the biochar coatings were not pure MgO. They were actually a mix of MgO and $MgCl_2$. The purity of MgO may be dependent on $MgCl_2$ concentration for the pretreatment and the production process. The particle size of the coated MgO on the corncob biochar was also variable in comparison to previous studies. These results suggest that the synthesis of MgO-coated biochar is sensitive to a range of factors (e.g., pre-treatment method, $MgCl_2$ concentration, protective gas during pyrolysis and pyrolysis temperature) and the process needs to be refined and verified to produce consistent materials that yield the expected results. Considering the significant improvement in reducing lead leachability and risks in the soil by the modification, such refinement and efforts are encouraged for future studies.

Long-term effectiveness is very important for stabilization-based remediation (Shen et al., 2018b). MgO generally has a stronger buffering capacity against acidic rain wash compared to biochar (Shen et al., 2018a; Shen et al., 2018c). It was observed in an accelerated ageing experiment simulating acidic rain wash that the immobilization of the same soil in this study by pure MgO remains effective 26 years after treatment (Shen et al., 2018c). The MgO treated soil just slightly exceeds TCLP regulatory level 52 years after treatment (Shen et al., 2018c). Therefore, the MgO coating can theoritically enhance the long-term performance of the biochar in soil remediation.

4. Conclusions

In this study, a magnesium oxide (MgO) coated corncob biochar was synthesized by pyrolyzing $MgCl_2$ pretreated corncob for a better performance in lead immobilization in a contaminated soil compared with corncob biochar. The properties and microstructures of CB and MCB were investigated. It was observed that MgO particles ranging from 1 to 2 μm were well coated on MCB, and the MgO content in MCB was calculated at 29.90%. The surface area of the biochar was significantly enhanced from 0.07 to 26.56 m^2/g after modification. The modification also significantly facilitated the lead removal percentage from 23% to 74% in aqueous solution by biochar. MCB was applied to a lead contaminated soil washing residue and resulted in a significant reduction in TCLP leached lead from 10.63 to 5.24 mg/L (reduced by 50.71%), whereas CB has no effects on lead immobilization in the soil. The comparison between MCB and other amendments suggests that the biochar component of MCB adsorbed lead onto its surface through cation-π interaction and increased surface adsorption due to higher surface area, and then the MgO coated on biochar's surface further enhanced the adsorption through precipitation.

Acknowledgements

This work was supported by the Opening Fund of National Engineering Laboratory for Site Remediation Technologies (No. NELSRT201702), and the National Water Pollution Control and Treatment Science and Technology Major Project (No. 2018ZX07109-003). Moreover, this study was partly funded by the Thousand Talents Plan of the Chinese government and Tsinghua University. The first author would like to thank the Killam Trusts of Canada for kindly providing the Izaak Walton Killam Memorial Postdoctoral Fellowship.

Appendix A. Supplementary data

Supplementary data to this article can be found online at https://doi.org/10.1016/j.envint.2018.11.045.

References

Alam, M.S., Gorman-Lewis, D., Chen, N., Flynn, S.L., Ok, Y., Konhauser, K., Alessi, D.S., 2018a. Thermodynamic analysis of nickel (II) and zinc (II) adsorption to biochar. Environ. Sci. Technol. https://doi.org/10.1021/acs.est.7b06261.

Alam, M.S., Swaren, L., von Gunten, K., Cossio, M., Bishop, B., Robbins, L.J., Hou, D., Flynn, S.L., Ok, Y.S., Konhauser, K.O., Alessi, D.S., 2018b. Application of surface complexation modeling to trace metals uptake by biochar-amended agricultural soils. Appl. Geochem. 88, 103–112. https://doi.org/10.1016/j.apgeochem.2017.08.003.

Al-Tabbaa, A., Liska, M., Ouellet-Plamondon, C., Jegandan, S., Shrestha, R., Barker, P., McGall, R., Critchlow, C., 2012. Soil mix technology for integrated remediation and ground improvement: from laboratory work to field trials. In: Grouting and Deep Mixing. 2012. pp. 522–532.

Bdewi, S.F., Abdulrazaka, A.M., Aziz, B.K., 2015. Catalytic Photodegradation of Methyl orange using MgO nanoparticles prepared by molten salt method. Asian Trans. Eng. 05.

Budai, A., Calucci, L., Rasse, D.P., Strand, L.T., Pengerud, A., Wiedemeier, D., Abiven, S., Forte, C., 2017. Effects of pyrolysis conditions on *Miscanthus* and corncob chars: characterization by IR, solid state NMR and BPCA analysis. J. Anal. Appl. Pyrolysis 128, 335–345. https://doi.org/10.1016/j.jaap.2017.09.017.

Hao, F., Zhao, X., Ouyang, W., Lin, C., Chen, S., Shan, Y., Lai, X., 2013. Molecular structure of corncob-derived biochars and the mechanism of atrazine sorption. Agron. J. 105, 773–782. https://doi.org/10.2134/agronj2012.0311.

Hou, D., Li, F., 2017. Complexities surrounding China's soil action plan. Land Degrad. Dev. 28, 2315–2320. https://doi.org/10.1002/ldr.2741.

Hou, D., O'Connor, D., Nathanail, P., Tian, L., Ma, Y., 2017a. Integrated GIS and multivariate statistical analysis for regional scale assessment of heavy metal soil contamination: A critical review. Environ. Pollut. 231, 1188–1200. https://doi.org/10.1016/j.envpol.2017.07.021.

Hou, D., Qi, S., Zhao, B., Rigby, M., O'Connor, D., 2017b. Incorporating life cycle assessment with health risk assessment to select the 'greenest' cleanup level for Pb contaminated soil. J. Clean. Prod. 162, 1157–1168. https://doi.org/10.1016/j.jclepro.2017.06.135.

Jin, F., Al-Tabbaa, A., 2014. Characterisation of different commercial reactive magnesia. Adv. Cem. Res. 26, 101–113.

Jung, K.W., Jeong, T.U., Hwang, M.J., Kim, K., Ahn, K.H., 2015. Phosphate adsorption ability of biochar/Mg-Al assembled nanocomposites prepared by aluminum-electrode based electro-assisted modification method with $MgCl_2$ as electrolyte. Bioresour. Technol. 198, 603–610. https://doi.org/10.1016/j.biortech.2015.09.068.

Keiluweit, M., Nico, P.S., Johnson, M.G., Kleber, M., 2010. Dynamic molecular structure of plant biomass-derived black carbon (biochar). Environ. Sci. Technol. 44, 1247–1253. https://doi.org/10.1021/es9031419.

Lehmann, J., 2007. Bio-energy in the black. Front. Ecol. Environ. preprint, 1. https://doi.org/10.1890/060133.

Lehmann, J., Skjemstad, J., Sohi, S., Carter, J., Barson, M., Falloon, P., Coleman, K., Woodbury, P., Krull, E., 2008. Australian climate–carbon cycle feedback reduced by

soil black carbon. Nat. Geosci. 1, 832–835. https://doi.org/10.1038/ngeo358.
Li, T., Bai, X., Qi, Y.X., Lun, N., Bai, Y.J., 2016. Fe_3O_4 nanoparticles decorated on the biochar derived from pomelo pericarp as excellent anode materials for Li-ion batteries. Electrochim. Acta 222, 1562–1568. https://doi.org/10.1016/j.electacta.2016.11.140.
Li, R., Wang, J.J., Zhou, B., Zhang, Z., Liu, S., Lei, S., Xiao, R., 2017. Simultaneous capture removal of phosphate, ammonium and organic substances by MgO impregnated biochar and its potential use in swine wastewater treatment. J. Clean. Prod. 147, 96–107. https://doi.org/10.1016/j.jclepro.2017.01.069.
Liu, W.J., Jiang, H., Tian, K., Ding, Y.W., Yu, H.Q., 2013. Mesoporous carbon stabilized MgO nanoparticles synthesized by pyrolysis of $MgCl_2$ preloaded waste biomass for highly efficient CO_2 capture. Environ. Sci. Technol. 47, 9397–9403. https://doi.org/10.1021/es401286p.
Liu, X., Zhang, Y., Li, Z., Feng, R., Zhang, Y., 2014. Characterization of corncob-derived biochar and pyrolysis kinetics in comparison with corn stalk and sawdust. Bioresour. Technol. 170, 76–82. https://doi.org/10.1016/j.biortech.2014.07.077.
Mosa, A., El-Ghamry, A., Tr??By, P., Omar, M., Gao, B., Elnaggar, A., Li, Y., 2016. Chemo-mechanical modification of cottonwood for Pb_{2+} removal from aqueous solutions: sorption mechanisms and potential application as biofilter in drip-irrigation. Chemosphere 161, 1–9. https://doi.org/10.1016/j.chemosphere.2016.06.101.
O'Connor, D., Peng, T., Zhang, J., Tsang, D.C.W., Alessi, D.S., Shen, Z., Bolan, N.S., Hou, D., 2018. Biochar application for the remediation of heavy metal polluted land: a review of in situ field trials. Sci. Total Environ. 619–620, 815–826. https://doi.org/10.1016/j.scitotenv.2017.11.132.
Qu, C., Shi, W., Guo, J., Fang, B., Wang, S., Giesy, J.P., Holm, P.E., 2016. China's soil pollution control: choices and challenges. Environ. Sci. Technol. 50, 13181–13183. https://doi.org/10.1021/acs.est.6b05068.
Sanderson, P., Naidu, R., Bolan, N., Lim, J.E., Ok, Y.S., 2015. Chemical stabilisation of lead in shooting range soils with phosphate and magnesium oxide: synchrotron investigation. J. Hazard. Mater. 299, 395–403. https://doi.org/10.1016/j.jhazmat.2015.06.056.
Shen, Z., McMillan, O., Jin, F., Al-Tabbaa, A., 2016a. Salisbury biochar did not affect the mobility or speciation of lead in kaolin in a short-term laboratory study. J. Hazard. Mater. 316, 214–220.
Shen, Z., Som, A.M., Wang, F., Jin, F., McMillan, O., Al-Tabbaa, A., 2016b. Long-term impact of biochar on the immobilisation of nickel (II) and zinc (II) and the re-vegetation of a contaminated site. Sci. Total Environ. 542, 771–776. https://doi.org/10.1016/j.scitotenv.2015.10.057.
Shen, Z., Zhang, Y., Jin, F., Mcmillan, O., Al-Tabbaa, A., 2017. Qualitative and quantitative characterisation of adsorption mechanisms of lead on four biochars. Sci. Total Environ. 609, 1401–1410. https://doi.org/10.1016/j.scitotenv.2017.08.008.
Shen, Z., Hou, D., Zhao, B., Xu, W., Ok, Y.S., Bolan, N.S., Alessi, D.S., 2018a. Stability of heavy metals in soil washing residue with and without biochar addition under accelerated ageing. Sci. Total Environ. 619–620, 185–193. https://doi.org/10.1016/j.scitotenv.2017.11.038.
Shen, Z., Li, Z., Alessi, D.S., 2018b. Stabilization-based soil remediation should consider long-term challenges. Front. Environ. Sci. Eng. 12. https://doi.org/10.1007/s11783-018-1028-9.
Shen, Z., Hou, D., Xu, W., Zhang, J., Jin, F., Zhao, B., Pan, S., Peng, T., Alessi, D.S., 2018c. Assessing long-term stability of cadmium and lead in a soil washing residue amended with MgO-based binders using quantitative accelerated ageing. Sci. Total Environ. 643, 1571–1578. https://doi.org/10.1016/j.scitotenv.2018.06.321.
Sizmur, T., Fresno, T., Akgül, G., Frost, H., Moreno-Jiménez, E., 2017. Bioresource technology biochar modification to enhance sorption of inorganics from water. Bioresour. Technol. https://doi.org/10.1016/j.biortech.2017.07.082.
Sohi, S.P., 2012. Carbon storage with benefits. Science 338, 1034–1035. https://doi.org/10.1126/science.1225987.
Suzuki, T., Nakamura, A., Niinae, M., Nakata, H., Fujii, H., Tasaka, Y., 2013. Lead immobilization in artificially contaminated kaolinite using magnesium oxide-based materials: immobilization mechanisms and long-term evaluation. Chem. Eng. J. 232, 380–387. https://doi.org/10.1016/j.cej.2013.07.121.
Upamali, A., Chen, S.S., Tsang, D.C.W., Zhang, M., Vithanage, M., Mandal, S., Gao, B., Bolan, N.S., Sik, Y., 2016. Engineered/designer biochar for contaminant removal/immobilization from soil and water: potential and implication of biochar modification. Chemosphere 148, 276–291. https://doi.org/10.1016/j.chemosphere.2016.01.043.
Von Gunten, K., Alam, S., Hubmann, M., Sik, Y., Konhauser, K.O., Alessi, D.S., 2017. Bioresource technology modified sequential extraction for biochar and petroleum coke: metal release potential and its environmental implications. Bioresour. Technol. 236, 106–110. https://doi.org/10.1016/j.biortech.2017.03.162.
Vu, T.M., Trinh, V.T., Doan, D.P., Van, H.T., Nguyen, T.V., Vigneswaran, S., Ngo, H.H., 2017. Removing ammonium from water using modified corncob-biochar. Sci. Total Environ. 579, 612–619. https://doi.org/10.1016/j.scitotenv.2016.11.050.
Wang, F., Jin, F., Shen, Z., Al-Tabbaa, A., 2016. Three-year performance of in-situ mass stabilised contaminated site soils using MgO-bearing binders. J. Hazard. Mater. 318, 302–307. https://doi.org/10.1016/j.jhazmat.2016.07.018.
Xin, O., Yitong, H., Xi, C., Jiawei, C., 2017. Magnetic biochar combining adsorption and separation recycle for removal of chromium in aqueous solution. Water Sci. Technol. 75, 1177–1184. https://doi.org/10.2166/wst.2016.610.
Yang, G.X., Jiang, H., 2014. Amino modification of biochar for enhanced adsorption of copper ions from synthetic wastewater. Water Res. 48, 396–405. https://doi.org/10.1016/j.watres.2013.09.050.
Zhang, F., Li, G., 2016. China released the action plan on prevention and control of soil pollution. Front. Environ. Sci. Eng. 10, 19.
Zhang, M., Gao, B., Yao, Y., Xue, Y., Inyang, M., 2012. Synthesis of porous MgO-biochar nanocomposites for removal of phosphate and nitrate from aqueous solutions. Chem. Eng. J. 210, 26–32. https://doi.org/10.1016/j.cej.2012.08.052.
Zhao, F.J., Ma, Y., Zhu, Y.G., Tang, Z., McGrath, S.P., 2015. Soil contamination in China: current status and mitigation strategies. Environ. Sci. Technol. 49, 750–759. https://doi.org/10.1021/es5047099.
Zhao, B., O'Connor, D., Zhang, J., Peng, T., Shen, Z., Tsang, D.C.W., Hou, D., 2017a. Effect of pyrolysis temperature, heating rate, and residence time on rapeseed stem derived biochar. J. Clean. Prod. 174, 977–987. https://doi.org/10.1016/j.jclepro.2017.11.013.
Zhao, S.X., Ta, N., Wang, X.D., 2017b. Effect of temperature on the structural and physicochemical properties of biochar with apple tree branches as feedstock material. Energies 10. https://doi.org/10.3390/en10091293.